Contents lists available at *Dergipark*

Journal of Scientific Reports-A

journal homepage: *https://dergipark.org.tr/tr/pub/jsr-a*

***E-ISSN: 2687-6167*** ***Number 57, June 2024***

***RESEARCH ARTICLE***

*Receive Date: 06.07.2023* *Accepted Date: 15.03.2024*

# Conway-Maxwell-Poisson profile monitoring with *rk*-Shewhart control chart: a comparative study

Ulduz MAMMADOVA[a]*

*Çukurova University, Faculty of Science and Letters, Department of Statistics, Adana, Türkiye, ORCID: 0000-0001-5022-4932*

**Abstract**

A control chart is an essential tool in Statistical Quality Control for monitoring the production process. It provides a visual means of identifying process irregularities. In this study, we focus on the Shewhart control chart based on the *rk*-deviance residuals, namely *rk*-Shewhart control charts to examine the Conway–Maxwell–Poisson (COM-Poisson) profile, which is used to model the count data with varying degrees of dispersion. The primary goal of this study is to identify the biasing parameter that produces the best result among newly presented biasing parameters developed based on existing ones. It provides a short overview of the COM-Poisson distribution, its modeling, and *rk* parameter estimation in the case of multicollinearity, as well as the construction of the deviance-residual-based Shewhart chart. To evaluate the performance of the *rk*-Shewhart, we conduct an analysis using a real-life data set, considering various shift sizes. By employing different biasing parameters, we examine the effectiveness of the *rk*-Shewhart control chart. The performance evaluation outcomes of the *rk*-Shewhart charts are compared to the *ML*-deviance-based Shewhart chart and within themselves based on the biasing parameters. The results demonstrate the advantage of the *rk*-Shewhart charts over the *ML*-deviance-based control chart in detecting out-of-control signals. Among the considered biasing parameters, the *rk*-Shewhart chart utilizing the adjusted biasing parameter $k_4$ shows the best performance based on the ARL metric.



*Keywords: Control chart; Conway-Maxwell-Poisson model; Multicollinearity; Process monitoring; rk estimation*

* Corresponding author
*E-mail address:* contact@ulduzmammadova.com

## 1. Introduction

Statistical process control covers a range of tools to examine the production process. One such tool is the control chart. Control charts allow visual inspection and quick identification of the irregularities in the process. The simplicity of the approach has made it attractive to researchers looking to develop new techniques to perform profile monitoring. The profile itself represents the quality of the product/process through a relationship between the response and one or more producers. An extreme similarity of profiles with regression models allows the implementation of the modeling methods into the monitoring. In cases with count response, the data from the process is generally regarded as the Poisson profile. Several studies are dedicated to monitoring Poisson profiles with predictors independent of each other [1] – [7] and with collinear relationship [8] – [10]. But Poisson distribution comes with the specific characterization of the data being equidispersed, in other words, having an equal mean-variance structure. The real-life data do not always fit under this structure by showing a higher mean than variance or vice versa. In the early 1960s, Conway and Maxwell [11] introduced the Conway – Maxwell – Poisson distribution, which can represent the count data with various levels of dispersion. The COM-Poisson distribution is reviewed in the generalized linear models (GLMs) framework by Guikema and Coffelt [12], Lord et al. [13], Jowaheer and Khan [14], and Sellers and Shmueli [15].

The possibility of modeling data with dispersed count response as GLM has led to the emergence of new studies in the context of process monitoring, as well. Inspired by Marcondes Filo and Sant'Anna [8], Park et al. [16] proposed an *R-control* chart based on the combination of regression modeling and principal component analysis, assuming the existence of interrelation among predictors. Later, Park et al. [17] introduced a randomized quantile residual-based control chart. Both studies are focused on monitoring process data with count response that follows Poisson, Negative Binomial, or COM-Poisson distributions. Mammadova and Özkale [9] adopted a different approach. For monitoring Poisson and COM-Poisson profiles, the authors used ridge estimation to lessen the effect of multicollinearity and proposed ridge-deviance-based Shewhart, cumulative sum (CUSUM), and exponentially weighted moving average (EWMA) charts. Jamal et al. [18] took a similar approach and studied deviance and randomized quantile residual-based CUSUM and EWMA charts for COM-Poisson process data and applied them to real-time highway safety surveillance. Mammadova and Özkale [9, 19, 20] also investigated COM-Poisson profile monitoring under multicollinearity by incorporating principal component regression (PCR), Liu, and *rk* estimation methods. Liu – deviance – based control charts proved to be better than the maximum likelihood (ML) and ridge deviance-based control charts, while *rk* deviance-based control charts outperformed ML, ridge, and PCR deviance-based control charts.

In this study, we mainly focused on the Shewhart control chart based on the *rk*-deviance residuals (*rk*-Shewhart). Unlike other methods, biased estimation methods require an optimal biasing parameter that provides an effective estimate without deviating far from its actual value. Since *the rk* estimation method combines PCR and ridge estimators, its value is also affected by the biasing parameter. In this paper, we evaluated the effect of the eight different biasing parameters of *k* on the overall performance of the control chart. The study aims to determine the best biasing parameter among considered ones that results in a good performance.

The rest of the paper is organized as follows: Section 2 covers detailed information about COM-Poisson modeling, an alternative estimation method of *rk* estimation, deviance residuals, and adjusted biasing parameters for *the rk* estimator as well. Monitoring with a residual-based Shewhart control chart is presented in Section 3. An illustrative example is included in Section 4, where the performance of the *rk*-Shewhart control chart with various biasing parameters is compared both among each other and to the performance of the *ML*-deviance-based Shewhart (*ML*-Shewhart) chart in general. Lastly, Section 6 covers the summary and conclusions regarding the study.

## 2. Conway-Maxwell-Poisson model

The probability density function for the COM-Poisson distribution is defined by

$$f(y_i) = \frac{\mu_i^{y_i}}{(y_i!)^{\nu}} \frac{1}{Z(\mu_i, \nu)}, i = 1,2,3, \dots, n \qquad \#(1)$$

where $y = 0,1,2, \dots$, $\nu$ is the dispersion parameter, and $Z(\mu_i, \nu) = \sum_{s=0}^{\infty} (\mu_i^s/(s!)^{\nu})$ is a normalization parameter. $\nu > 1$ indicates an underdispersion and $\nu < 1$ shows that data is overdispersed. $\nu = 1$ is the equidispersed case.

The distribution is known to have three special cases, which are Geometric (when $\nu = 0, \mu_i < 1$), Poisson (when $\nu = 1$), and Bernoulli (when $\nu \to \infty$) distributions. According to Shmueli et al. [21], the normalization parameter $Z(\mu_i, \nu)$ does not converge when $\nu = 0$ and $\mu_i \geq 1$. Consequently, the distribution is undefined in that case.

As GLM, data with COM-Poisson distributed response is commonly modeled through the log-link function [12, 14, 15]. The log-link function of $\mu_i = exp(x_i\beta)$ involves $i$th observation $x_i = [x_{i1}, x_{i2}, \dots, x_{ip}]$ of $X_{n\times p} = [x_1, x_2, \dots, x_n]'$ predictor matrix and unknown $\beta = [\beta_1, \beta_2, \dots, \beta_p]'$ parameters. In the case of independent predictors, these unknown parameters can be estimated iteratively by using the *ML* estimation technique as

$$\hat{\beta}_{ML}^{(t)} = \left(X'\hat{V}_{ML}^{(t-1)}X\right)^{-1} X'\hat{V}_{ML}^{(t-1)}\hat{u}_{ML}^{(t-1)} \qquad \#(2)$$

where *t* indicates the iteration step, $\hat{u}_{ML}^{(t-1)} = X\hat{\beta}_{ML}^{(t-1)} + \left(\hat{V}_{ML}^{(t-1)}\right)^{-1}\left(y - \hat{\mu}_{ML}^{(t-1)}\right)$ is the working response, and $\hat{V}_{ML}$ is the weight matrix evaluated at $\hat{\beta}_{ML}^{(t-1)}$. The *ML* estimator at convergence is $\hat{\beta}_{ML} = \left(X'\hat{V}_{ML}X\right)^{-1}X'\hat{V}_{ML}\hat{u}_{ML}$ . Francis et al. [22] presented a general form of the weight matrix $\hat{V}_{ML}$ for *ML* estimation, initially given by Sellers and Shmueli [15]. It can be calculated as in Appendix A.

The presence of the correlation among predictors requires the utilization of alternative estimation methods. One such method is the *rk* estimation. Initially, the *rk* estimator was proposed by Baye and Parker [23] for linear models and later modified for GLMs by Abbasi and Özkale [24]. To obtain the *rk* estimator first, we perform singular value decomposition to determine the principle components as follows:

Let $X^* = XT$ and $\alpha = T'\beta$, where $T = [t_1, t_2, \dots, T_p]$ is the $p \times p$ orthogonal matrix through $T'X'\hat{V}_{ML}XT = \Lambda$. $\Lambda = diag(\lambda_i), i = 1,2, \dots, p$, and $\lambda_i$ are the eigenvalues of the $X'\hat{V}_{ML}X$ matrix. While $\lambda_1$ is equivalent to the maximum eigenvalue, $\lambda_p$ is the minimum. Then linear predictor in canonical form can be written as $\eta = X\beta = XTT'\beta = X^*\alpha$ and $X^* = [X_r^* X_{p-r}^*]$ where $X_r^* = XT_r$ $(r \leq p)$ is the matrix of principal components that corresponds to the large eigenvalues and $r$ is the number of principal components that will be in the model. Accordingly, $\omega, T,$ and $\Lambda$ can be partitioned as $\alpha = [\alpha_r\ \alpha_{p-r}], T = [T_r\ T_{p-r}]$, and $\Lambda = \begin{bmatrix} \Lambda_r & 0 \\ 0 & \Lambda_{p-r} \end{bmatrix}$, where $\Lambda_r = T_r'X'\hat{V}_{ML}XT_r$ and $\Lambda_{p-r} = T_{p-r}'X'\hat{V}_{ML}XT_{p-r}$, respectively.

The number of principal components can be determined via the metric proposed by Jollife [25] called the percentage of the total variance (PTV). In this study, we adopted the adjusted version of this metric for GLMs, introduced by Aguilera [26], where $PTV = \left(\sum_{i=1}^{r}\hat{\lambda}_i/\sum_{i=1}^{p}\hat{\lambda}_i\right) \times 100\%$.

Mammadova and Özkale [20] obtained *rk* estimator for COM-Poisson model as

$$\hat{\beta}_{rk}^{(t)} = T_r\left(T_r'X'\hat{V}_{ML}^{(t-1)}XT_r + kI_r\right)^{-1}T_rX'\hat{V}_{ML}^{(t-1)}\hat{u}_{rk}^{(t-1)} \qquad (3)$$

where $k$ is the biasing parameter and $\hat{u}_{rk}^{(t-1)} = XT_rT_r'\hat{\beta}_{rk}^{(t-1)} + \left(\hat{V}_{ML}^{(t-1)}\right)^{-1}\left(y - \hat{\mu}_{rk}^{(t-1)}\right)$ is the working response. The $\hat{\beta}_{rk}$ estimator at convergence is as $\hat{\beta}_{rk} = T_r\left(T_r'X'\hat{V}_{ML}XT_r + kI_r\right)^{-1}T_rX'\hat{V}_{ML}\hat{u}_{rk}$. When $k = 1$, $\hat{\beta}_{rk}$ is the same as PCR estimator.

Once parameters are estimated, we can calculate deviance residuals. Sellers and Shmueli [15] defined the $i$th deviance-residual (*ML*-deviance) formula for the COM-Poisson model where the *ML* estimation method is utilized as

$$d_{ML,i} = \pm \left[2\left(L(y_i, y_i; v) - L\left(\hat{\mu}_{ML,i}, y_i; v\right)\right)\right]^{1/2} \tag{4}$$

where $L(y_i, y_i; v) = \sum_{i=1}^{n} y_i \, log(y_i) - v \sum_{i=1}^{n} log(y_i!) - \sum_{i=1}^{n} log(Z(y_i; v))$ is the log-likelihood function of the saturated model, and $L\left(\hat{\mu}_{ML,i}, y_i; v\right) = \sum_{i=1}^{n} y_i \log\left(\hat{\mu}_{ML,i}\right) - v \sum_{i=1}^{n} \log(y_i!) - \sum_{i=1}^{n} \log\left(Z\left(\hat{\mu}_{ML,i}; v\right)\right)$ is the log-likelihood of the fitted model. When $y_i < \hat{\mu}_{ML,i}$ the sign of the residual is negative, otherwise it is positive.

Mammadova and Özkale [20] modified Eq. (4) and obtained the *i*th *rk*-deviance residual as follows

$$d_{rk} = \pm \left[2\left(L(y_i, y_i; v) - L\left(\hat{\mu}_{rk,i}, y_i; v\right)\right)\right]^{1/2} \tag{5}$$

where $L\left(\hat{\mu}_{rk,i}, y_i; v\right) = \sum_{i=1}^{n} y_i \, log\left(\hat{\mu}_{rk,i}\right) - v \sum_{i=1}^{n} log(y_i!) - \sum_{i=1}^{n} log\left(Z\left(\hat{\mu}_{rk,i}; v\right)\right)$ is the log-likelihood of the fitted model where the *rk* estimation method is applied. Similarly, the sign of the residual is negative if $y_i < \hat{\mu}_{rk,i}$ and positive when $y_i \geq \hat{\mu}_{rk,i}$.

### *2.1. Biasing parameter k*

The possibility of obtaining the *rk* estimator simply by adjusting ridge biasing parameters was mentioned by Abbasi and Özkale [24]. The literature contains numerous studies on the choice of the biasing parameter *k* for ridge estimation. Hoerl and Kennard [27] and Hoerl et al. [28] presented the early biasing parameters. Several studies focused on the *k* parameters for linear ridge regression [29] – [34] and eventually, the biasing parameters proposed in these studies adapted to GLMs. [9], [10], [35] –[39] examined the *k* parameters of models with count response and carried out comparative studies to determine the optimal *k*. One of the recent studies, Kibria [40] reviewed more than a hundred bias parameters for GLM.

Here we present some of the biasing parameters adjusted for the *rk* estimation of COM-Poisson model parameters considered in this paper:

$$k_1 = \frac{v}{(\max(\hat{\alpha}_i))^2} \tag{6}$$

$$k_2 = \frac{rv}{\sum_{i=1}^{r} \alpha_i^2} \tag{7}$$

$$k_3 = \max\left(1/\sqrt{v/\,\hat{\alpha}_i^2}\right) \tag{8}$$

$$k_4 = median\left(\sqrt{v/\,\hat{\alpha}_i^2}\right) \tag{9}$$

$$k_5 = \max\left(\frac{v}{\hat{\alpha}_i^2} + \frac{1}{\lambda_i}\right) \tag{10}$$

$$k_6 = \text{median}\left(\frac{v}{\hat{\alpha}_i^2} + \frac{1}{\lambda_i}\right) \tag{11}$$

$$k_7 = \min\left(1/\sqrt{\frac{max(\lambda_i v)}{(n-r-1)v + \lambda_{max}\hat{\alpha}_i^2}}\right) \tag{12}$$

$$k_8 = \text{median}\left(1/\sqrt{\frac{max(\lambda_i v)}{(n-r-1)v + \lambda_{max}\hat{\alpha}_i^2}}\right) \tag{13}$$

where $\lambda_i$ is the eigenvalue of the $T_r'X'V_{ML}XT_r$ matrix.

The formulations for $k_1$ and $k_2$ in Eqs. (6) and (7) are based on the biasing parameters introduced by Hearl and Kennard [27] and Hearl et al. [28], respectively. These biasing parameters, known for their simplicity and adaptability, represent the earliest contributions to the literature, establishing a foundation for the development of new biasing parameters for more thorough analysis. $k_3$ and $k_4$ are obtained based on the recommendations of Muniz and Kibria [31]. Kibria et al. [36] stated that the earlier version of the $k_3$ is particularly efficient when high correlation is present among predictors for Poisson ridge estimation. The biasing parameters donated as $k_5$ and $k_6$ derived from the two biasing parameters presented by Alkhamisi and Shukur [30] for linear models. They have proven to produce the best results for Poisson profile monitoring by Mammadova and Özkale [10] in the framework of process control. The final two biasing parameters originated from the biasing parameters for COM-Poisson regression model presented by Sami et al. [39]. The authors suggested using those biasing parameters to overcome the multicollinearity issue based on the findings of the extensive simulation study.

## 3. Monitoring procedure

In the 1920s, the Shewhart control chart was introduced to the literature as a method to detect abnormalities in the production process caused by various factors [41]. In the following years, these control charts have undergone modifications and adjustments to be able to monitor different process data. In the profile monitoring framework, residuals derived from profiles are monitored through the Shewhart control chart to detect process irregularities assuming that residuals follow the normal distribution. Since deviance residuals derived from GLMs are proven to be closer to the normal distribution than Pearson residuals [42] – [43], most of the studies employed deviance residuals for monitoring generalized linear profiles with Shewhart control charts.

Shewhart control chart based on the deviance residuals can be constructed by using the following control limits

$$LCL = \mu_{ML,0} - L\sigma_{ML,0} \tag{14}$$

$$UCL = \mu_{ML,0} + L\sigma_{ML,0} \tag{15}$$

where *LCL* is the lower and *UCL* is the upper control limit, *L* is the width of the limits, $\mu_{ML,0}$ and $\sigma_{ML,0}$ are the mean and standard deviation of the *ML*-deviance residuals under an in-control state, respectively. Any observation outside of the control limits indicates an out-of-control state. Following the same approach, Mammadova and Özkale [44] obtained control limits for the *rk*-Shewhart control chart as

$$\boldsymbol{LCL = \mu_{rk,0} - L\sigma_{rk,0}} \tag{16}$$

$$\boldsymbol{UCL = \mu_{rk,0} + L\sigma_{rk,0}} \tag{17}$$

where $\mu_{rk,0}$ and $\sigma_{rk,0}$ are the in-control mean and standard deviation of the *rk*-deviance residuals, respectively.

The $L$ value in the control limits for the Shewhart control chart may differ slightly depending on the data set. It is typically selected based on the desired in-control average run length (*ARL*), which is the average number of data points until the first out-of-control signal. It is usually set to $ARL_0 \approx 370$. This choice ensures a minimal false alarm rate of 0.0027.

## 4. Illustrative example

### *4.1. Data set and its initial examination*

The comprehensive evaluation of the performances of the control charts is carried out through the SECOM data set [45]. The SECOM data set involves a collection of sensor readings, corresponding test results obtained from the production line, and a precise date-time stamp for each data point. While data from 590 sensors is considered a predictor matrix, test results act as the response.

To ensure that the data set fit the presumptions of the study, we performed data cleaning procedures. These include addressing missing values by replacing them with the previous value and reducing the number of predictors by removing non-continuous variables. Also, given that the response variable is binary (-1 for Pass, 1 for Failure), we rearranged the whole data set to be able to model it with the COM-Poisson regression model. The strategy for rearrangement is given below:

a) Following the cleaning, the initial predictor matrix became $X_{1567\times444}$.
b) Based on the time stamp, the 24 hours are divided into eight distinct time intervals, referred to as time frames (TF). Time frames are

| | |
|---|---|
| 1 → 00:00-02:59, | 2 → 03:00-05:59, |
| 3 → 06:00-08:59, | 4 → 09:00-11:59, |
| 5 → 12:00-14:59, | 6 → 15:00-17:59, |
| 7 → 18:00-20:59, | 8 → 21:00-23:59. |

A new date-time-frame (DTF) column was created by joining TF with the date information. For instance, the DTF of "20-5-2008-2" is the category of the observations for 20th May of 2008 and the time period between 03:00-05:59.
c) A rearranged response is created by summing the number of passes in the respective DTF. Similarly, the corresponding predictors are calculated by averaging each predictor variable within the corresponding DTF. Consequently, the data set became consist of $X_{476\times444}$ predictor matrix and a $Y_{476\times1}$ response vector of counts.
d) Lastly, to ensure the presence of multicollinearity, predictors with the absolute pairwise correlation value between [0.744, 0.756] are selected to be included in the analysis. Only 30 predictors met this condition. The final data set is a matrix of $X_{476\times30}$ and vector of $Y_{476\times1}$.

A further application is performed following the workflow given by Figure 1.

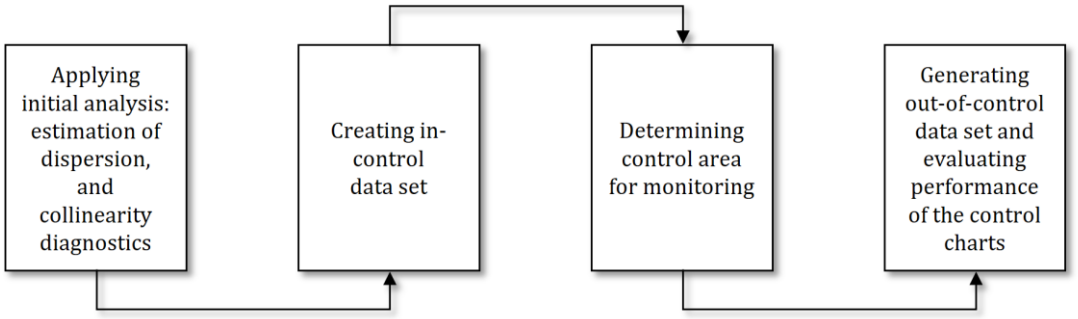


Figure 1. Application process workflow.

Prior to the analysis, we standardized the *X* matrix such that each column has a zero mean and unit variance. The estimation of the dispersion is carried out using the *"COMPoissonReg"* package [46], where $\nu = 0.7772$ is obtained, reflecting overdispersion.

Next, we model the relationship between the overdispersed response and predictors through the log-link function. The *ML* estimator is obtained iteratively, with the initial value being the ordinary least squares estimator. The convergence criterion is set as $||\hat{\beta}^{(t)} - \hat{\beta}^{(t-1)}|| \leq 10^{-6}$. In the final iteration, we calculated the weight matrix $\hat{V}_{ML}$ together with the *ML* estimator. Then condition number donated as *CN* is calculated by taking the square root of the maximum eigenvalue divided by the minimum eigenvalue of the scaled information matrix to assess collinearity among predictors. The result $CN = 237.2906 > 10$ indicates the presence of severe collinearity among the predictors according to Mackinnon and Puterman [47].

### *4.2. Monitoring and performance evaluation*

For the monitoring process, first, we computed $d_{ML}$ and $d_{rk}$ residuals. The $d_{rk}$ residuals are obtained from models where the model parameters are estimated using *rk* estimation with the respective biasing parameter. These estimators are calculated iteratively by setting $PTV = 95\%$, $\hat{\beta}^0 = T_r T_r'(X'X)^{-1}X'y$ as the initial value, and $||\hat{\beta}^{(t)} - \hat{\beta}^{(t-1)}|| \leq 10^{-6}$ as convergence criterion. The biasing parameters are calculated according to Eqs. (6) - (13) and obtained as $k_1 = 9.4355, k_2 = 23.1216, k_3 = 0.00042, k_4 = 77.3809, k_5 = 170.9183, k_6 = 68.2304, k_7 = 2.3757$, and $k_8 = 2.9525$.

Next, we conducted a preliminary analysis because of the absence of information regarding the state of the data set. A control area is established using the estimated mean and standard deviation of residuals to identify potential out-of-control data points outside $3\sigma$ control area. The control area is determined based on the estimated standard deviation of the monitored observations using the control limits in Eqs. (14)-(17). Resulted control charts are presented in Figure 2.

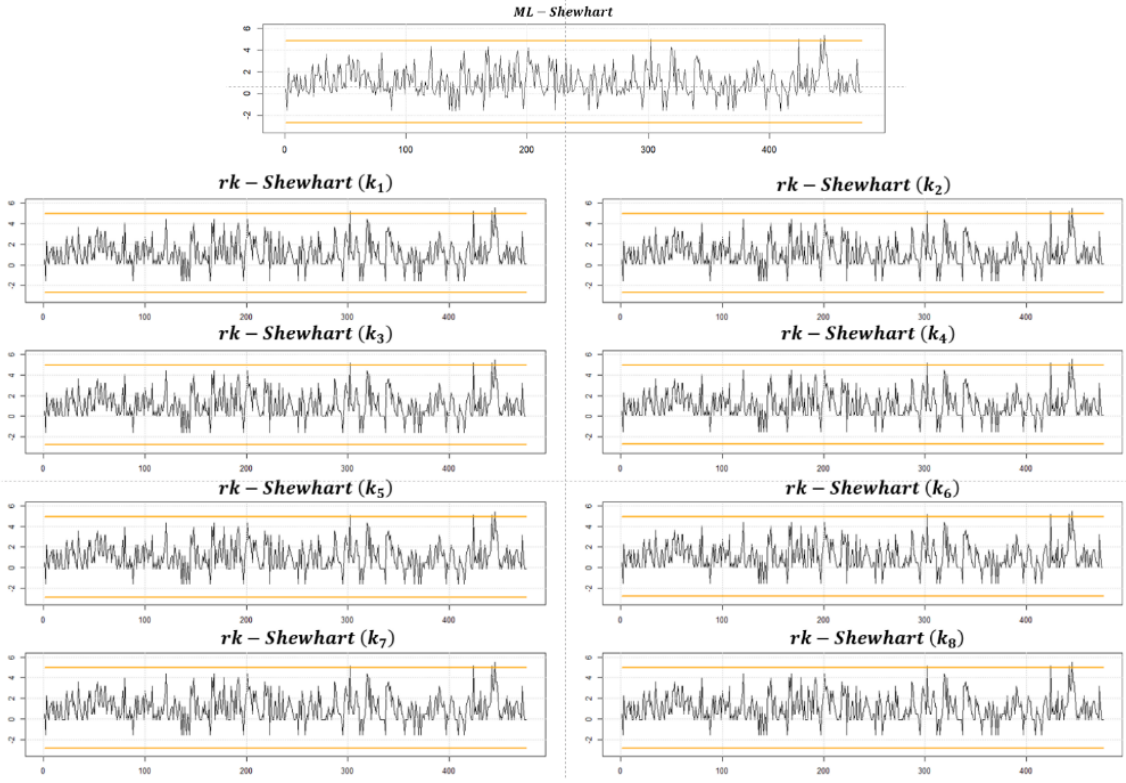


Figure 2. Initial analysis of the SECOM data set with ML-Shewhart and *rk*-Shewhart control charts.

Four unique data points (302nd, 424th, 442nd, 445th) fall outside the control area of all control charts. These observations are eliminated from the data matrix to create an in-control data set. Afterward, the model is refitted using the updated data set. New biasing parameters are obtained as $k_1 = 11.9482, k_2 = 25.9485, k_3 = 0.00039, k_4 = 58.6119, k_5 = 133.3645, k_6 = 53.6406, k_7 = 2.4283$ and $k_8 = 2.9115$. Then, the model parameters are estimated using the same settings, and residuals are calculated accordingly. Lower and upper control limits for the *ML*-Shewhart and *rk*-Shewhart control charts are obtained as in Eqs. (14) - (17) through simulation using these residuals such that they met the condition of $ARL_0 \approx 370$.

The simulation-derived control limits are included in Table 1.

Table 1. Control limits of the *ML*-Shewhart and *rk*-Shewhart control charts obtained through simulation.

| Control chart | LCL | UCL |
|---|---|---|
| *ML*-Shewhart | -3.425 | 2.870 |
| *rk*-Shewhart($k_1$) | -3.228 | 2.660 |
| *rk*-Shewhart($k_2$) | -3.282 | 2.710 |
| *rk*- | - | 2. |

| | | |
|---|---|---|
| Shewhart($k_3$) | 3.027 | 724 |
| *rk*- | - | 2. |
| Shewhart($k_4$) | 3.267 | 747 |
| *rk*- | - | 2. |
| Shewhart($k_5$) | 3.138 | 830 |
| *rk*- | - | 2. |
| Shewhart($k_6$) | 3.286 | 904 |
| *rk*- | - | 2. |
| Shewhart($k_7$) | 3.286 | 779 |
| *rk*- | - | 2. |
| Shewhart($k_8$) | 3.408 | 848 |

To be able to evaluate the performance of the control charts, we generate a shifted response $y \sim COM - Poisson(\mu_1, v)$, where $\mu_1 = exp(x_i\hat{\beta}_{ML} + \delta\hat{\sigma}_{ML,0})$, $\delta$ represents the shift size, and $\hat{\sigma}_{ML,0}$ donates the standard deviation of the in-control $d_{ML}$. The $\delta = 0.5,1,1.5,2,2.5,3$ is considered for a detailed evaluation of the effect of the biasing parameters on the monitoring process. Once the shifted response is generated, we modeled the relationship between predictors and response, estimated the model parameters using the same biasing parameters, and calculated the residuals. Then we compared these residuals to the control limits and calculated $ARL_1$ following [48]. The results are presented in Table 2.

According to Table 2, regardless of the shift size, the *rk*-Shewhart control chart outperformed the *ML*-Shewhart control chart in terms of $ARL_1$. The *rk*-Shewhart control chart with biasing parameter $k_4$ is the best-performing control chart among *rk* – deviance – based charts. It is followed by *rk*-Shewhart($k_2$) when $\delta > 0.5$. Also, with an increase in shift size, the control chart performances show noticeable improvements.

Table 2. Performance of the *ML*-Shewhart and *rk*-Shewhart control charts.

| Control chart | $\delta = 0$ | $\delta = 0.5$ | $\delta = 1$ | $\delta = 1.5$ | $\delta = 2$ | $\delta = 2.5$ | $\delta = 3$ |
|---|---|---|---|---|---|---|---|
| *ML*-Shewhart | 370.746 | 202.478 | 54.540 | 17.329 | 7.050 | 3.605 | 2.242 |
| *rk*-Shewhart($k_1$) | 370.628 | 194.907 | 52.437 | 16.874 | 6.898 | 3.558 | 2.215 |
| *rk*-Shewhart($k_2$) | 372.410 | 179.159 | 45.839 | 15.083 | 6.235 | 3.275 | 2.057 |
| *rk*-Shewhart($k_3$) | 371.176 | 197.257 | 52.023 | 16.754 | 6.868 | 3.546 | 2.201 |
| *rk*-Shewhart($k_4$) | 371.969 | 169.111 | 44.550 | 14.728 | 6.058 | 3.213 | 2.035 |
| *rk*-Shewhart($k_5$) | 370.591 | 176.780 | 48.756 | 15.782 | 6.478 | 3.365 | 2.117 |
| *rk*-Shewhart($k_6$) | 370.059 | 190.232 | 51.820 | 16.661 | 6.816 | 3.508 | 2.186 |
| *rk*-Shewhart($k_7$) | 369.995 | 177.014 | 47.400 | 15.420 | 6.356 | 3.315 | 2.091 |
| *rk*-Shewhart($k_8$) | 370.460 | 186.037 | 50.242 | 16.296 | 6.645 | 3.453 | 2.152 |

## 5. Conclusions

This research focuses on the variations of the *rk*-Shewhart control chart for detecting unexpected deviations in the COM-Poisson profile. This monitoring method employs deviance residuals derived from a model with parameters estimated via the *rk* estimation method. Given that the *rk* estimation method integrates PCR and ridge estimators, the choice of biasing parameter influences its performance. In this study, we aimed to investigate the impact of the set of biasing parameters on the performance of the *rk*-Shewhart control chart and determine the one that yields optimal performance of the control chart.

We reviewed eight distinct biasing parameters from the literature and adjusted them to the COM-Poisson profile for *rk* estimation. The impact of biasing parameters for the COM-Poisson profile is evaluated using a real-life data set. It is modified to reflect the study's assumptions, and shifts in various sizes are added for a thorough comparison. The performance of each *rk*-Shewhart control chart is evaluated and in addition to being compared among themselves, the performance of the *rk*-Shewhart charts is also compared to that of the *ML*-Shewhart chart.

Findings revealed that the *rk*-Shewhart control chart consistently outperforms the deviance-based Shewhart control chart, regardless of the chosen biasing constant. The superiority of the *rk*-Shewhart control chart indicates an elevated sensitivity in detecting deviations in the process mean. In particular, the *rk*-Shewhart chart based on the biasing parameter $k_4$, as proposed by Muniz and Kibria [31], demonstrates the best performance among all control charts regarding the *ARL* metric.

In conclusion, the study highlights the superior performance of the *rk*-Shewhart control chart, particularly when adapted to the COM-Poisson profile with adjusted biasing parameters. The findings show the importance of modifying statistical procedures for best performance in a variety of data scenarios.

For future research an investigation of additional biasing parameters to improve the effectiveness of the control charts utilizing the *rk* estimation method may be considered. Furthermore, the implementation of advanced statistical techniques and machine learning algorithms can provide more comprehensive and effective process monitoring.

## Acknowledgements

The author would like to thank anonymous reviewers for their valuable feedback and suggestions, which enhanced the quality of this paper.

Author ORCID ID: https://orcid.org/0000-0001-5022-4932

## References

[1] K.R. Skinner, D.C. Montgomery, and G.C. Runger, "Process monitoring for multiple count data using generalized linear model-based control charts," *Int. J. Prod. Res.*, vol. 41, no. 6, pp. 1167–1180, Jun. 2003, doi: 10.1080/00207540210163964.

[2] K.R. Skinner, D.C. Montgomery, and G.C. Runger, "Generalized linear model-based control charts for discrete semiconductor process data," *Qual. Reliab. Eng. Int.*, vol. 20, no. 8, pp. 777–786, 2004, doi: 10.1002/qre.603.

[3] D. Jearkpaporn, D.C. Montgomery, G.C. Runger, and C.M. Borror, "Process monitoring for correlated gamma-distributed data using generalized-linear-model-based control charts," *Qual. Reliab. Eng. Int.*, vol. 19, no. 6, pp. 477–491, 2003, doi: 10.1002/qre.521.

[4] A. Amiri, M. Koosha, and A. Azhdari, "Profile monitoring for Poisson responses," in *IEEE Int. Conf. Ind. Eng. Eng. Manag.*, 2011, pp. 1481–1484, doi: 10.1109/IEEM.2011.6118163

[5] A. Asgari, A. Amiri, and S.T.A. Niaki, "A new link function in GLM-based control charts to improve monitoring of two-stage processes with Poisson response," *Int. J. Adv. Manuf. Technol.*, vol. 72, no. 9, pp. 1243–1256, 2014, doi: 10.1007/s00170-014-5692-z.

[6] W.Y. Hwang, "Quantile-based control charts for Poisson and gamma distributed data," *J. Korean Stat. Soc.*, pp. 1–18, 2021, doi: 10.1007/s42952-021-00108-6.

[7] H. Wen, L. Liu, and X. Yan, "Regression-adjusted Poisson EWMA control chart," *Qual. Reliab. Eng. Int.*, vol. 37, no. 5, pp. 1956–1964, 2021, doi: 10.1002/qre.2840.

[8] D. Marcondes Filho and A.M.O. Sant'Anna, "Principal component regression – based control charts for monitoring count data," *Int. J. Adv. Manuf. Technol.*, vol. 85, no. 5, pp. 1565–1574, 2016, doi: 10.1007/s00170-015-8054-6.

[9] U. Mammadova and M.R. Özkale, "Profile monitoring for count data using Poisson and Conway – Maxwell – Poisson regression–based control charts under multicollinearity problem," *J. Comput. Appl. Math.*, vol. 388, p. 113275, 2021, doi: 10.1016/j.cam.2020.113275.

[10] U. Mammadova and M.R. Özkale, "Comparison of deviance and ridge deviance residual-based control charts for monitoring Poisson profiles," *Commun. Stat. – Simul. Comput.*, vol. 52, no. 3, pp. 826–853, 2023, doi: 10.1080.

[11] R.W. Conway and W.L. Maxwell, "A queuing model with state-dependent service rates," *J. Ind. Eng.*, vol. 12, no. 2, pp. 132–136, 1962. [Online]. Available: https://tinyurl.com/28cv3brs

[12] S.D. Guikema and J.P. Coffelt, "A flexible count data regression model for risk analysis," *Risk Anal.: An Int. J.*, vol. 28, no. 1, pp. 213–223, 2008, doi: 10.1111/j.1539-6924.2008.01014.x.

[13] D. Lord, S.D. Guikema, and S.R. Geedipally, "Application of the Conway–Maxwell–Poisson generalized linear model for analyzing motor vehicle crashes," *Accident Anal. & Prev.*, vol. 40, no. 3, pp. 1123–1134, 2008, doi: 10.1016/j.aap.2007.12.003.

[14] V. Jowaheer and N.M. Khan, "Estimating regression effects in COM–Poisson generalized linear model," *Int. J. Comput. Math. Sci.*, vol. 1, no. 2, pp. 59-63, 2009, doi: 10.5281/zenodo.1075883.
[15] K.F. Sellers and G. Shmueli, "A flexible regression model for count data," *Ann. Appl. Stat.*, vol. 4, no. 2, pp. 943–961, 2010, doi: 10.2139/ssrn.1127359
[16] K. Park, J.M. Kim, and D. Jung, "GLM-based statistical control r-charts for dispersed count data with multicollinearity between input variables," *Qual. Reliab. Eng. Int.*, vol. 34, no. 6, pp. 1103–1109, 2018, doi: 10.1002/qre.2310.
[17] K. Park, D. Jung, and J.M. Kim, "Control charts based on randomized quantile residuals," *Appl. Stoch. Models Bus. Ind.*, vol. 36, no. 4, pp. 716–729, 2020, doi: 10.1002/asmb.2527.
[18] A. Jamal et al., "GLM-based flexible monitoring methods: An application to real-time highway safety surveillance," *Symmetry*, vol. 13, no. 2, p. 362, 2021, doi: 10.3390/sym13020362.
[19] U. Mammadova and M.R. Özkale, "Conway–Maxwell Poisson regression-based control charts under iterative Liu estimator for monitoring count data," *Appl. Stoch. Models Bus. Ind.*, vol. 38, no. 4, pp. 695-725, 2022, doi: 10.1002/asmb.2682.
[20] U. Mammadova and M.R. Özkale, "Detecting shifts in Conway–Maxwell–Poisson profile with deviance residual-based CUSUM and EWMA charts under multicollinearity," *Stat. Papers*, pp. 1–47, 2023, doi: 10.1007/s00362-023-01399-z.
[21] G. Shmueli, T.P.Minka, J.B. Kadane, S. Borle, and P. Boatwright, "A useful distribution for fitting discrete data: revival of the Conway–Maxwell–Poisson distribution," *J. R. Stat. Soc.: Series C (Appl. Stat.)*, vol. 54, no. 1, pp. 127–142, 2005, doi: 10.1111/j.1467-9876.2005.00474.x.
[22] R.A. Francis, S.R. Geedipally, S.D. Guikema, S.S. Dhavala, D. Lord, and S. LaRocca, "Characterizing the performance of the Conway-Maxwell-Poisson generalized linear model," *Risk Anal.: An Int. J.*, vol. 32, no. 1, pp. 167–183, 2012, doi: 10.1111/j.1539-6924.2011.01659.x.
[23] M.R. Baye and D.F. Parker, "Combining ridge and principal component regression: a money demand illustration," *Commun. Stat.-Theory Methods*, vol. 13, no. 2, pp. 197–205, 1984, doi: 10.1080/03610928408828675.
[24] A. Abbasi and M.R. Özkale, "The r-k class estimator in generalized linear models applicable with sim. and empirical study using a Poisson and gamma responses," *Hacettepe J. Math. Stat.*, vol. 50, no. 2, pp. 594–611, 2021, doi: 10.15672/hujms.715206.
[25] I.T. Jolliffe, Principal Components in Regression Analysis. New York: Springer, 2002.
[26] A.M. Aguilera, M. Escabias, and M.J. Valderrama, "Using principal components for estimating logistic regression with high-dimensional multicollinear data," *Comput. Stat. Data Anal.*, vol. 50, no. 8, pp. 1905–1924, 2006, doi: 10.1016/j.csda.2005.03.011.
[27] A.E. Hoerl and R.W. Kennard, "Ridge regression: Biased estimation for nonorthogonal problems," *Technometrics*, vol. 12, no. 1, pp. 55–67, 1970, doi: 10.2307/1267351.
[28] A.E. Hoerl, R.W. Kannard, and K.F. Baldwin, "Ridge regression: some simulations," *Commun. Stat.-Theory Methods*, vol. 4, no. 2, pp. 105–123, 1975, doi: 10.1080/03610927508827232.
[29] B.M.G. Kibria, "Performance of some new ridge regression estimators," *Commun. Stat.-Simulation Comput.*, vol. 32, no. 2, pp. 419–435, 2003, doi: 10.1081/SAC-120017499.
[30] M.A. Alkhamisi and G. Shukur, "A Monte Carlo study of recent ridge parameters," *Commun. Stat.-Simulation Comput.*, vol. 36, no. 3, pp. 535–547, 2007, doi: 10.1080/03610910701208619.
[31] G. Muniz and B.M.G. Kibria, "On some ridge regression estimators: An empirical comparison," *Commun. Stat.-Simulation Comput.*, vol. 38, no. 3, pp. 621–630, 2009, doi: 10.1080/03610910802592838.
[32] Y. Asar, A. Karaibrahimoglu, and G. Aşır, "Modified ridge regression parameters: A comparative Monte Carlo study," *Hacettepe J. Math. Stat.*, vol. 43, no. 5, pp. 827–841, 2014. [Online]. Available: https://dergipark.org.tr/en/pub/hujms/issue/43879/536843
[33] Y. Asar and A. Genç, "A note on some new modifications of ridge estimators," *Kuwait J. Sci.*, vol. 44, no. 3, 2017. [Online]. Available: https://journalskuwait.org/kjs/index.php/KJS/article/view/1110
[34] M. Qasim et al., "Biased adjusted Poisson ridge estimators – method and application," *Iran. J. Sci. Technol. Trans. A Sci.*, vol. 44, pp. 1775–1789, 2020, doi: 10.1007/s40995-020-00974-5.
[35] K. Mansson and G. Shukur, "A Poisson ridge regression estimator," *Econ. Model.*, vol. 28, no. 4, pp. 1475–1481, 2011, doi: 10.1016/j.econmod.2011.02.030.
[36] B.M.G. Kibria, K. Mansson, and G. Shukur, "A simulation study of some biasing parameters for the ridge type estimation of Poisson regression," *Commun. Stat.-Simulation Comput.*, vol. 44, no. 4, pp. 943–957, 2015, doi: 10.1080/03610918.2013.796981.
[37] A. Zaldivar, "On the performance of some Poisson ridge regression estimators" (Master's thesis). Florida International University, 2018, doi: 10.25148/etd.fidc006538.
[38] Z.Y. Algamal and M.M. Alanaz, "Proposed methods in estimating the ridge regression parameter in Poisson regression model," *Electron. J. Appl. Stat. Anal.*, vol. 11, no. 2, pp. 506–515, 2018,
doi: 10.1285/i20705948v11n2p506.
[39] F. Sami, M. Amin, and M.M. Butt, "On the ridge estimation of the Conway–Maxwell–Poisson regression model with multicollinearity: Methods and applications," *Concurrency Comput. Pract. Exp.*, vol. 34, no. 1, e6477, 2022, doi: 10.1002/cpe.6477.
[40] B.M.G. Kibria, "More than hundred (100) estimators for estimating the shrinkage parameter in a linear and generalized linear ridge regression models," *J. Econom. Stat.*, vol. 2, no. 2, pp. 233–252, 2022, doi: 10.47509/JES.2022.v02i02.06.
[41] W.A. Shewhart, "Some applications of statistical methods to the analysis of physical and engineering data," *Bell Syst. Tech. J.*, vol. 3, no. 1, pp. 43–87, 1924, doi: 10.1002/j.1538-7305.1924.tb01347.x.
[42] D.A. Pierce and D.W. Schafer, "Residuals in generalized linear models," *J. Am. Stat. Assoc.*, vol. 81, no. 396, pp. 977–986, 1986, doi: 10.1080/01621459.1986.10478361.
[43] T. Park, C.S. Davis, and N. Li, "Alternative GEE estimation procedures for discrete longitudinal data," *Comput. Stat. Data Anal.*, vol. 28, no. 3, pp. 243–256, 1998, doi: 10.1016/s0167-9473(98)00039-5.

[44] U. Mammadova and M.R. Özkale, "Deviance residual-based Shewhart control chart for monitoring Conway-Maxwell-Poisson profile under the r-k class estimator," *Qual. Tech. Quan. Manag.* pp. 1-22, 2023, doi: 10.1080/16843703.2023.2259589.
[45] M. McCann and A. Johnston, "Dataset: SECOM." *UC Irvine Machine Learning Repository*, https://archive.ics.uci.edu/dataset/179/secom.
[46] K. Sellers, T. Lotze, A. Raim, and M.A. Raim, "COMPoissonReg (R package version 3.0)." *A comprehensive R archieve network*, https://cran.r-project.org/web/packages/COMPoissonReg/index.html
[47] M.J. Mackinnon and M.L. Puterman, "Collinearity in generalized linear models," *Commun. Stat.-Theory Methods*, vol. 18, no. 9, pp. 3463–3472, 1989, doi: 10.1080/03610928908830102.
[48] D.C. Montgomery, Introduction to Statistical Quality Control. John Wiley & Sons, New Jersey, 2012.

## Appendix A. Weight matrix

$$V_{ML} = diag\left(\sum_{s=0}^{\infty}\frac{\left[\frac{v(v-1)s^2\left(exp\left(\mu_{i,ML}\right)\right)^{2s}\left(\frac{\left(exp\left(\mu_{i,ML}\right)\right)^{s}}{s!}\right)^{v-2}}{(s!)^2}+\frac{vs^2(exp(\mu_i))^{s}\left(\frac{\left(exp\left(\mu_{i,ML}\right)\right)^{s}}{s!}\right)^{v-1}}{s!}\right]}{\sum_{s=0}^{\infty}\left(\frac{\left(exp\left(\mu_{i,ML}\right)\right)^{s}}{s!}\right)^{v}}\right.$$

$$\left.-\sum_{s=0}^{\infty}\frac{\left[\frac{vs\left(exp\left(\mu_{i,ML}\right)\right)^{s}\left(\frac{\left(exp\left(\mu_{i,ML}\right)\right)^{s}}{s!}\right)^{v-1}}{(s!)^2}\right]^2}{\sum_{s=0}^{\infty}\left(\frac{\left(exp\left(\mu_{i,ML}\right)\right)^{s}}{s!}\right)^{2v}}\right)$$